Available online at www.elixirpublishers.com (Elixir International Journal)

Nanotechnology

Elixir Nanotechnology 107 (2017) 47326-47331

ISSN: 2229-712X

Pectin based ZnO Nanocomposite Hydrogel: Evaluation as Adsorbent for Divalent Metal Ions from Aqueous Solutions

Arun Krishna K. and Vishalakshi B.*

Department of Post-Graduate Studies & Research in Chemistry, Mangalore University, Mangalagangothri-574199 (DK), Karnataka, India.

ARTICLE INFO

Article history:
Received: 26April 2017;
Received in revised form:
12 June 2017;
Accepted: 24 June 2017;

Keywords
Nanocomposite hydrogel,
Pectin,
Microwave,
ZnO nanoparticles,
Metal adsorption.

ABSTRACT

Synthesis of a nanocomposite hydrogel P-PAMPS-PAAm/ZnO has been done by the polymerization of 2-acrylamido-2-methyl-1-propanesulfonic acid (AMPS) and acrylamide (AAm) in the presence of pectin (P) and zinc oxide (ZnO) using microwave irradiation technique. FTIR, XRD, SEM and TEM studies indicated the formation of a gel network and incorporation of ZnO particles within gel structure. The system was evaluated for adsorption of Cu (II) and Pb(II) ions from aqueous solutions. About 77 mg/g of Cu(II) and 125 mg/g of Pb(II) could be adsorbed from aqueous solutions. Different isotherm models have been employed to study the adsorption process and the data is found to fit well with Langmuir isotherm model. The kinetic studies revealed a second-order adsorption process. About 95% of the metal ions adsorbed could be stripped in acidic medium of pH 1.2 indicating the reusability of the gel.

1. Introduction

Variety of anthropogenic activities results in pollution of water by different means. One among them is pollution by heavy metals. Heavy metals are those metallic elements whose density is greater 5.0g/cm^3 and are toxic at very low concentration.

Industrial processes, combustion of fossil-fuels, waste incineration and disposal, transportation and agricultural activities etc are some of the ways through which these metals get into the environment (1).

Heavy metals are toxic substances which are persistent and bio-accumulative (2). Copper salts are extensively used for the galvanization of metals, as fungicides, fertilizers, anti-fouling agents etc which causes serious health problems to the aquatic as well as terrestrial living organisms. High concentration of copper can lead to cancer in human beings (3). The same way presence of lead can cause serious effects to human beings, such as cancer, dizziness, renal failure, etc (4) and (5).

Various techniques such as chemical precipitation, membrane filtration, coagulation and ion exchange have been employed for the treatment of polluted water. While the limitation such as poor performance, low efficiency for the adsorption of metals, lack of selectivity and high cost have made most of these processes impractical (6). Recently nanomaterials have emerged as efficient adsorbents for the treatment of water contaminated with heavy metals.

Recently Chitosan-Montmorillonite Composite (7), chitosan modified with β-cyclodextrin (8), Chitosan/Polyvinyl alcohol/Zeolite composite (9), thiacalix[4]arenetetrasulfonate-functionalized reduced graphene oxide (5), Montmorillonite-Humic acid-Bacteria Composites (10), Fe_3O_4 embedded ZnO nanocomposites (11), kaolinite-supported zero-valent iron nanoparticles (12), sodium alginate-polyaniline nanofibers (13), etc have been used for the adsorption of various metal ions from aqueous solutions.

In this investigation, we describe a ternary polymeric network system embedded with ZnO nanoparticles for the removal of copper and lead ions from aqueous solutions. Many polymeric systems have been used widely for the removal of heavy metal ions from waste water. The purpose of this study was to design a system with great adsorption capacity. Here in this study polysaccharide was linked with monomeric units containing anionic groups which can improve the metal ion adsorption property. More adsorption sites were provided by the incorporation of nanoparticles. Fit of kinetic data into the pseudo-first-order and pseudo-second-order models were also investigated; while the appropriate adsorption isotherm was identified by applying the Langmuir and Freundlich isotherms. Further, the desorption capacity of the nanocomposite hydrogel was investigated to determine the long term reusability of the nanocomposite hydrogels.

2. Experimental Sections

2.1 Chemicals and reagents

All the chemicals used for the experiments were analytical grade reagents. Pectin (P) and 2-acrylamido-2-methyl-1-propanesulfonic acid (AMPS) were obtained from Sigma Aldrich Chemical Company, India. Acrylamide (AAm) and sodium hydroxide were obtained from Loba Chemie, India. N,N′-methylene-bis-acrylamide (MBA), ammonium peroxodisulphate (APS), copper sulphate and lead nitrate were obtained from Spectrochem Pvt. Ltd., Mumbai, India. Zinc sulfate was obtained from Thermo Fisher Scientific India Pvt. Ltd., India. Potassium chloride (KCl) was purchased from Merck, India. Hydrochloric acid was obtained from NICE chemicals, Kochi, India. Double distilled water was used in all experiments.

Tele: +91-824-2287262
E-mail address: vishalakshi2009@yahoo.com

2.2 Methods

2.2.1 Synthesis of zinc oxide (ZnO) nanoparticles

ZnO nanoparticles were synthesized as reported previously (14). Aqueous sodium hydroxide was added drop wise to the aqueous zinc sulfate solution in a molar ratio 1:2 under vigorous stirring at room temperature. Stirring was continued for 12 hours and the resulting solution was then filtered, washed with deionized water. The precipitate obtained was dried in a hot air oven at 100 ºC for 12 hours.

2.2.2 Microwave assisted synthesis of novel pectin-poly (2-acrylamido-2-methyl-1-propanesulfonic acid)-polyacrylamide (P-PAMPS-PAAm) and its ZnO nanocomposite (P-PAMPS-PAAm/ZnO) gel

A mass of 0.05 g pectin was dissolved in 15 ml water and stirred overnight to get homogeneous solution. To this solution, previously made ZnO nanoparticles (0.002 g) were added and sonicated for the homogeneous dispersion of the nanoparticles in solution. Added 0.15 g AMPS followed by 0.4 g acrylamide, 0.015 g APS and 0.1002 g MBA under stirring and the stirring was continued for 3 hours. Microwave (80 W) was then passed through the mixture for 25 seconds. The obtained gel was transferred to acetone taken in a beaker and kept overnight to remove the unreacted monomers. It was then purified in methanol and dried in a hot air oven at 50 ^{o}C for 24 hours. P-PAMPS-PAAm was made by the same procedure but without the addition of ZnO.

2.3 Characterization techniques

2.3.1 Fourier Transform Infrared Spectroscopy (FTIR)

FTIR spectra of P-PAMPS-PAAm and P-PAMPS-PAAm/ZnO were recorded on a FTIR spectrometer Shimadzu IR Prestige 21 (Japan) in transmittance mode in the range of 500 cm^{-1} to 4000 cm^{-1}.

2.3.2 Scanning Electron Microscopy (SEM)

Morphological study of P-PAMPS-PAAm and P-PAMPS-PAAm/ZnO was carried out by recording the SEM images using JEOL-JSM5800LV (Japan) Scanning electron microscope. The micrographs were recorded with different magnifications.

2.3.3 Thermo gravimetric analysis (TGA)

TGA of P-PAMPS-PAAm and P-PAMPS-PAAm/ZnO were recorded on the thermogravimetric analyser SDT Q600 V20.9 (Japan). The samples were heated from room temperature to 700 ^{o}C under nitrogen atmosphere at a rate of 10 ^{o}C/min.

2.3.4 X-Ray Diffraction (XRD)

Powder X-ray diffraction pattern of ZnO, P-PAMPS-PAAm and P-PAMPS-PAAm/ZnO were recorded using benchtop X-ray diffractometer, Rigaku MiniFlex 600 (Japan). The diffraction pattern is recorded at an angle range of 0^{o} to 80^{o} at room temperature at the recording of 2^{o}/minute.

2.3.5 Transmission Electron Microscopy (TEM)

The presence and size of nanoparticles were confirmed using JEOL/JEM 2100 transmission electron microscope (USA) operating at 200 kV.

2.4 Adsorption and desorption studies

2.4.1 Metal adsorption

The capacity of nanocomposite hydrogel, P-PAMPS-PAAm/ZnO to extract divalent metal ions from aqueous solution was carried out by batch process using two divalent metal ions, namely, Cu(II) and Pb(II). About 10 mg of P-PAMPS-PAAm/ZnO was suspended in 10.0 mL of aqueous solution of each metal ion with concentrations varying from 20 to 200 mg/L. After 2 hours the suspensions were centrifuged and the concentration of the metal ions in the supernatant solution was determined by using GBC 932 Plus Atomic Absorption Spectrophotometer (Australia). The absorption capacity of the gel sample was determined using the following equation

$$Q_e = (C_i - C_e) \times \frac{V}{m} \quad (1)$$

Where C_i is the initial metal concentration (mg/L), C_e is the residual metal concentration at equilibrium (mg/L), V is the volume of solution (L) and m is the amount (g) of dry gel samples used for adsorption studies.

2.4.2 Metal desorption

To check the reusability of adsorbent materials, adsorption experiments were followed by desorption studies. About 10.0 mg of the sample was suspended in metal solutions of initial concentrations 200 mg/L. After 2 hours, the gel loaded with metal ions was separated by centrifugation, washed with water and dried. About 10.0 mg of adsorbed sample was suspended in 10 mL of stripping solution of pH 1.2 (prepared using HCl). The solution was stirred for 2 hours at room temperature and centrifuged. Aliquot of the solution was taken and concentration of the desorbed metal ion was determined by AAS. The percentage of desorption (D) was calculated using the following equation,

$$D\ (\%) = \frac{Amount\ of\ M^{+}\ desorbed}{Amount\ of\ M^{+}\ adsorbed} \times 100 \quad (2)$$

where M^{+} is metal ion

3. Results and Discussion

3.1Microwave assisted synthesis of P-PAMPS-PAAm/ZnO nanocomposite

Under the influence of microwave dielectric heating, the generation of free radicals from the initiators facilitates the formation of pectin macroradicals RO· which acts as the radical sites for graft copolymerization. The incorporation of tetrafunctional monomer MBA in the grafted chains leads to crosslinked structure. The mechanism of formation of the three dimensional network structure is shown in Fig. 1. The nanoparticles will be dispersed at the free space in the gel network.

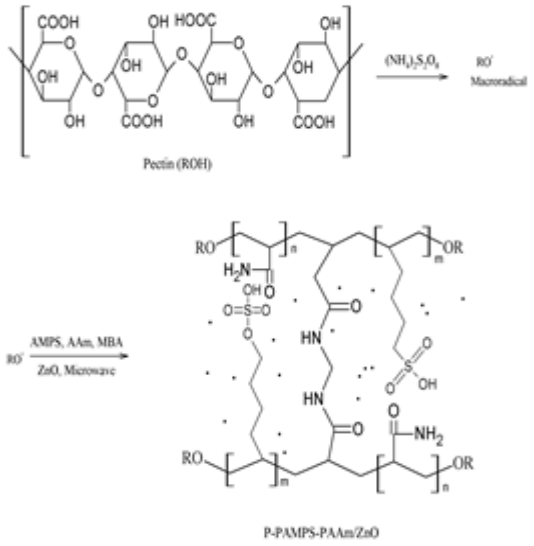

Figure 1. Mechanism of formation of P-PAMPS-PAAm/ZnO nanocomposite hydrogel.

3.2 FTIR Spectroscopy

FTIR spectra of P-PAMPS-PAAm and P-PAMPS-PAAm/ZnO are displayed in Fig. 2. Peaks between 3250-3500 cm^{-1} are due to the –OH and NH stretching of pectin, AMPS and AAm respectively.

The peak at 1685 cm^{-1} is due to the C=O stretching of pectin. The S=O stretching of AMPS occurs at 1040 cm^{-1} and the additional peak in Fig. 2b at 670 cm^{-1} and 555 cm^{-1} are due to the stretching vibrations of Zn-O bonds.

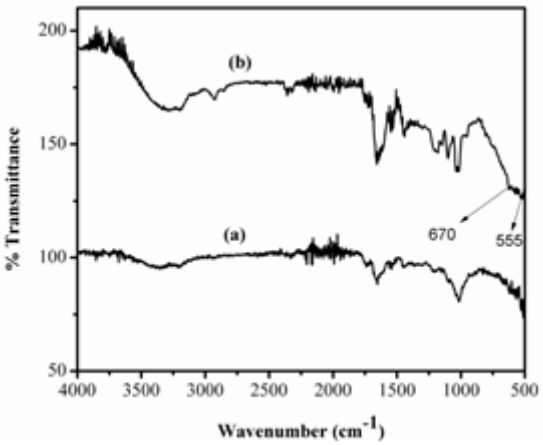

Figure 2. FTIR spectra of (a) P-PAMPS-PAAm and (b) P-PAMPS-PAAm/ZnO.

3.3 Thermogravimetric analysis

The thermogravimetric curves for the P-PAMPS-PAAm gel and its nanocomposite, P-PAMPS-PAAm/ZnO are shown in Fig. 3. The former gel shows three stage degradation, while the nanocomposite degrades by multiple steps. In the first stage of degradation, P-PAMPS-PAAm loses water between 25 ºC to 100 ºC. Second step degradation occurs between 200-400ºC which is due to the decomposition of polysaccharide backbone. The third and last degradation starts at a temperature 400 ºC and proceeds gradually. Complete degradation of the system can be observed at 620 ºC. The first step degradation starts from 25 ºC to 300 ºC which is due to dehydration of the sample. The second step degradation starts at 420 ºC till 672 ºC. The nanocomposite hydrogel shows similar degradation pattern except the gradual loss of water in the first stage and a complete loss of weight at a higher temperature of 720 ºC.

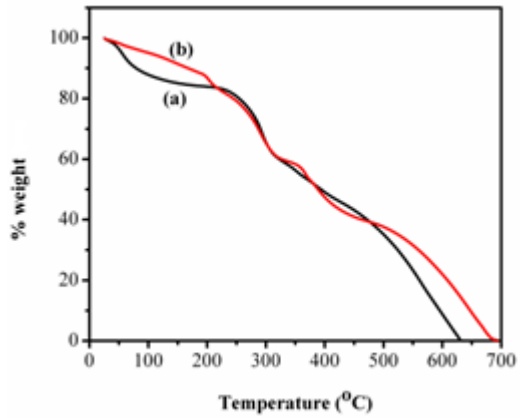

Figure 3. Thermograms of (a) P-PAMPS-PAAm and (b) P-PAMPS-PAAm/ZnO.

3.4 X-Ray Diffraction

Fig. 4 displays the XRD pattern of P-PAMPS-PAAm, pure ZnO and P-PAMPS-PAAm/ZnO nanocomposite. The amorphous nature of P-PAMPS-PAAm is evident from the broad XRD pattern (Fig. 4a). The sharp crystalline peaks of ZnO nanoparticles observed at different 2θ values ranging from 30º to 80º in Fig. 4b are also observed in the nanocomposite hydrogel (Fig. 4c) confirming the presence of crystalline ZnO nanoparticles in the gel matrix.

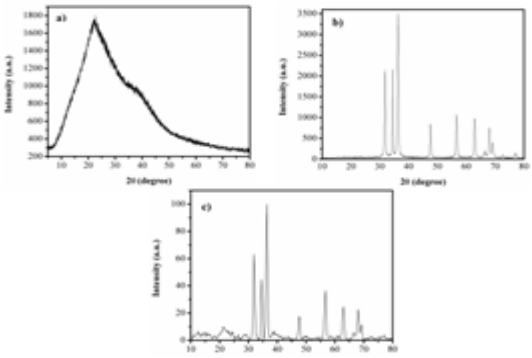

Figure 4. X-ray diffraction pattern of (a) P-PAMPS-PAAm, (b) ZnO nanoparticles and (c) P-PAMPS-PAAm/ZnO.

3.5 SEM analysis

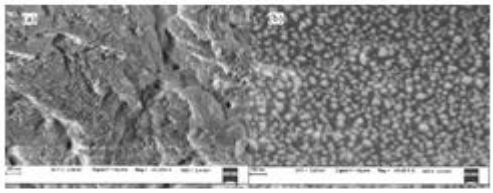

Figure 5. SEM images of (a) P-PAMPS-PAAm and (b) P-PAMPS-PAAm/ZnO.

The porous, non-homogeneous surface of P-PAMPS-PAAm (Fig. 5a) drastically changes on incorporation of ZnO. The P-PAMPS-PAAm/ZnO samples show a smoothened surface with homogeneous distribution of spherical ZnO nanoparticles (Fig. 5b).

3.6 TEM analysis

High resolution TEM analysis confirms the spherical nature of the ZnO nanoparticles embedded within the interpenetrating network system (Fig. 6a) and Fig. 6b shows the electron diffraction pattern of where two diffraction rings are clearly visible for the nanoparticles.

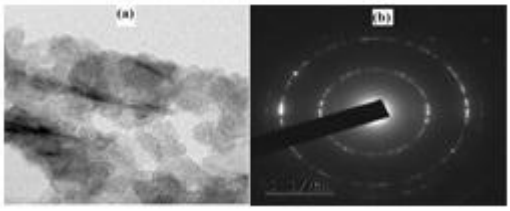

Figure 6a. TEM image of P-PAMPS-PAAm/ZnO (b) Electron Diffraction Pattern.

3.7 Metal adsorption studies

The nanocomposite hydrogel was studied for its capacity to adsorb divalent metal ions from aqueous solutions by taking Cu(II) and Pb(II) salt solutions. The batch adsorption process was carried out in neutral pH at room temperature. The carboxylate group of pectin and the sulfonate group of PAMPS act as binding sites for electrostatic interaction of metal cations and the primary amine groups of PAAm bind to metal cations via coordinate bonds.

3.7.1 Adsorption isotherm studies

The nature of adsorption between solid and liquid phase can be explained with the help of isotherm models. In this work, we have examined the adsorption process using two adsorption isotherm models, namely the Langmuir (15) and Freundlich (16) models.

The Langmuir isotherm is based on the assumption that the solid surface provides uniform and identical sites for adsorption and there is no interaction between adsorbed species.

That is, the adsorbed amount has no influence on rate of adsorption and there occur a monolayer formation of adsorbate molecules on the surface of adsorbent. The linear form of Langmuir isotherm is,

$$\frac{C_e}{Q_e} = \frac{1}{q_m} C_e + \frac{1}{q_m K_L} \quad (3)$$

where 'Q_e' is the amount of metal ions adsorbed per unit mass of adsorbent at equilibrium (mg/g), 'C_e' is the concentration of metal ions in solution at equilibrium (mg/L), 'q_m' is the maximum amount of adsorbate corresponding to complete monolayer coverage on the adsorbent surface (mg/g), and 'K_L' is the Langmuir constant.

The essential characteristics of the Langmuir isotherm can be expressed in terms of a dimensionless constant R_L (17), which is given by the following equation

$$R_L = \frac{1}{1+K_L C_0} \quad (4)$$

The parameter R_L indicates the nature of adsorption as given below.

$R_L > 1$	Unfavourable adsorption
$0 < R_L > 1$	Favourable adsorption
$R_L = 0$	Irreversible adsorption
$R_L = 1$	Linear adsorption

Freundlich adsorption isotherm is described as a non-ideal reversible isotherm model and it is not restricted to monolayer formation. This model can be applied to the multilayer adsorption. The mathematical expression representing this model is,

$$Q_e = K_F C_e^{1/n} \quad (5)$$

Logarithmic form of above equation is more compatible for plotting the graph, which is given as,

$$\log Q_e = \log K_F + \frac{1}{n} \log C_e \quad (6)$$

where 'Q_e' and 'C_e' have their usual meaning and 'K_F' and 'n' indicate the extent of the adsorption and the degree of nonlinearity between the solution concentration and the adsorbate, respectively. These constants are known as Freundlich adsorption isotherm constants. K_F and n can be calculated from the intercept and slope of the plot between 'log Q_e' and 'log C_e'. Adsorption can be considered as favourable only if the value of 'n' lies between 1 and 10.

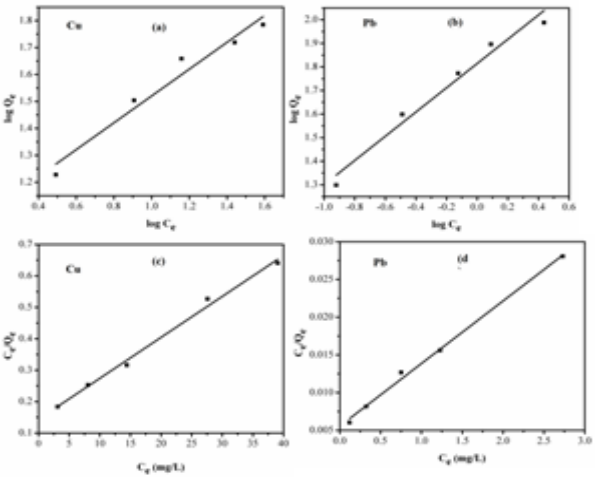

Figure 7. Freundlich [(a) & (b)] and Langmuir [(c) & (d)] plots for adsorption of Cu & Pb on P-PAMPS-PAAm/ZnO.

Table 1. Adsorption parameters of Cu(II) and Pb(II) on P-PAMPS-PAAm/ZnO.

Metal	Langmuir model				Freundlich model		
	R_L	K_L	R^2	q_m (mg/g)	K_F	n	R^2
Cu(II)	0.099	0.09	0.99	76.92	10.52	2.01	0.96
Pb(II)	0.005	1.60	0.99	125.0	65.16	1.95	0.96

The high value of regression coefficient, R^2, in case of Langmuir isotherm model fit indicates that the adsorption of both the metal ions can be defined by Langmuir isotherm model. The adsorption capacity of the gel sample is found to be 76.92 mg of Cu and 125 mg of Pb per gram of adsorbent respectively.

3.7.2 Adsorption kinetics

Kinetics of the adsorption process was tested by employing Lagergren'pseudo-first-order model' (15) and the Ho 'pseudo-second order model' (18).

Fixed amount (10.0 mg) of adsorbent and 10 mL of 200 mg/L adsorbate solution were used for the kinetic studies. The mathematical representation for Lagergren'pseudo-first-order model' is given as

$$\frac{dQ_t}{d_t} = k_1(Q_e - Q_t) \quad (7)$$

Integrating the above equation and noting that Q_t =0 when t= 0

$$\log(Q_e - Q_t) = \log Q_t - \frac{k_1 t}{2.303} \quad (8)$$

where Q_e has its usual meaning, Q_t is the amount of dye adsorbed per unit of adsorbent (mg/g) at time t, k_1 is the pseudo-first-order rate constant (min^{-1}), and 't' is the contact time (min). The Q_e and k_1 values are calculated from the intercept and slope of the plot of log (Q_e- Q_t) v/s t (not shown) and are presented in Table 2.

Representation of Ho 'pseudo-second order' model is as follows

$$\frac{dQ_t}{d_t} = k_2(Q_e - Q_t)^2 \quad (9)$$

On integrating the above equation with boundary conditions, Q_t = 0 at t = 0, we get,

$$\frac{t}{Q_t} = \frac{1}{k_2 Q_e^2} + \frac{t}{Q_e} \quad (10)$$

where k_2 is the pseudo-second order rate constant (g/mg/min). The initial adsorption rate, h is defined as

$$h = k_2 Q_e^2 \quad (11)$$

The values of 'Q_e', 'k_2' and 'h' are obtained from the linear plot of 't/Q_t' v/s 't'. The values of Q_e, k_2 and h are given in table 2.

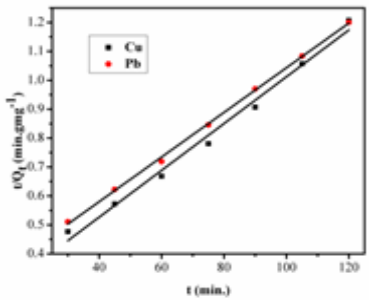

Figure 8. Pseudo-second order plot for the metal ions Cu and Pb.

Table 2. Study of pseudo first order and pseudo second order kinetic parameters for the adsorption process.

Metal	$Q_{e,exp}$	Pseudo-first order			Pseudo-second order			
	(mg/g)	Q_e (mg/g)	k_1 (min^{-1})	R^2	Q_e (mg/g)	k_2 (g/mg/min)	h (mg/g/min)	R^2
Cu	126.00	841.4	0.083	0.93	125.00	0.0003	5.0	0.99
Pb	162.22	102.8	0.029	0.98	142.86	0.0002	3.59	0.99

3.8 Desorption

Desorption experiments were carried out with single metal (Cu/Pb) loaded samples. Aqueous buffer solution of pH 1.2 was used as the stripping solution as the adsorbents have zero affinity for metal ions under acidic conditions. At this pH the carboxylic group and sulphate groups get protonated and lose their affinity toward metal ions, thus release them to the solution. The results of adsorption and desorption experiments are shown in Fig. 8. About 95 % Cu and 97 % Pb adsorbed by the gel could be released in one desorption cycle.

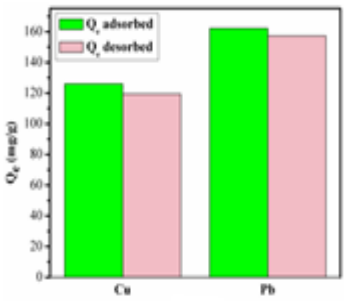

Figure 9. Amount of metal ions adsorbed and desorbed (Qe).

3.9 Comparison of the performance of the nanocomposite hydrogel with other adsorbents

Adsorption efficiency of P-PAMPS-PAAm/ZnO for Cu and Pb ions has been compared with other systems that are reported previously. The maximum amount of metal adsorbed and the material used for the ad sorption process are given in the following table.

Table 3. Comparison of adsorption capacity of P-PAMPS-PAAm/ZnO with other reported materials.

Adsorbent	Q_{max} (mg/g)		References
	Cu(II)	Pb(II)	
Ethylenediamine modified chitosan microspheres	60.97	46.51	(19)
Ethylenediamine modified chitosan	32.30	28.57	(20)
Watermelon rind	-	55.0	(21)
Silica-Bipyridine Framework	64.84	99.68	(22)
Porcellanite	3.49	24.38	(23)
PMMA core–surfactin shell nanoparticles	80.0	86.0	(24)
α-Fe_2O_3/PAN nanofiber mat	-	81.97	(25)
Palm shell activated carbon	1.581	1.337	(26)
Chitosan-Montmorillonite Composite	34.91	-	(7)
Chitosan-PAA-graphene oxide beads	-	138.89	(4)
P-PAMPS-PAAm/ZnO	76.92	125	Present work

4. Conclusion

The novel nanocomposite hydrogel, P-PAMPS-PAAm/ZnO was made using microwave irradiation technique. The chemical and surface structure of the gel has been established. The nanocomposite gel is found to have good capacity to adsorb divalent metal ions such as Cu and Pb from solutions and the adsorption capacity is found to be 77 mg/g of Cu(II) and 125 mg/g of Pb(II) which is the highest when compared to other already reported systems.

The adsorption process is found to fit well with the pseudo-second order kinetic model. The adsorption isotherms of the system have been found to follow Langmuir model. Further the desorption studies indicated that most of the adsorbed metal ions get desorbed in the striping solution of pH 1.2. Hence, the present study reveals that the P-PAMPS-PAAm/ZnO nanocomposite system can be considered as a promising adsorbent for removal of the divalent metal ions from aqueous solutions.

References

1. Di Natale, F., Erto, A., Lancia, A., Musmarra, D., "A descriptive model for metallic ions adsorption from aqueous solutions onto activated carbons." Journal of Hazardous Materials, 2009, Vol. 169, pp. 360–369.

2. Cocarta, A. I., Gutanu, V., Dragan, E. S., "Comparative Sorption of Co^{2+}, Ni^{2+} and Cr^{3+} onto Chitosan/Poly(vinyl amine) Composite Beads." Cellulose Chemistry and Technology, 2015, Vol. 49, pp. 775-782.

3. Schmuhl, R., Krieg, H. M., Keizer, K., "Adsorption of Cu(II) and Cr(VI) ions by chitosan: kinetics and equilibrium studies." Water SA, 2001, Vol. 27, pp. 1-8.

4. Medina, R. P., Nadres, E. T., Ballesteros Jr., F. C., Rodrigues, D. F., "Incorporation of graphene oxide into a chitosan–poly(acrylic acid) porous polymer nanocomposite for enhanced lead adsorption." Environmental Science: Nano, 2016, Vol. 3, pp. 638-646.

5. Liu, C., Zhang, D., Zhao, L., Lu, X., Zhang, P., He, S., Hu, G., Tang, X., "Synthesis of a thiacalix[4]arenetetrasulfonate functionalized reduced graphene oxide adsorbent for the removal of lead(II) and cadmium(II) from aqueous solutions." RSC Advances, 2016, Vol. 6, pp. 113352–113365.

6. Gan, M., Zheng, Z., Sun, S., Zhu, J., Liu, X., "The influence of aluminum chloride on biosynthetic schwertmannite and Cu(II)/Cr(VI) adsorption." RSC Advances, 2015, Vol. 5, pp. 94500-94512.

7. Hu, C., Hu, H., Zhu, J., Deng, Y., Li, C., "Adsorption of Cu^{2+} on Montmorillonite and Chitosan-Montmorillonite Composite toward Acetate Ligand and the pH Dependence." Water, Air and Soil Pollution, 2016, Vol. 227, pp. 1-10.

8. Sharma, A. K., and Mishara, A. K., "Microwave induced beta-cyclodextrin modification of chitosan for lead sorption." International Journal of Biological Macromolecules, 2010, Vol. 47, pp. 410-419.

9. Habibaa, U., Siddiqueb, T. A., Jooa, T. C., Salleha, A., Anga, B. C., Afifi, A. M., "Synthesis of chitosan/polyvinyl alcohol/zeolite composite for removal of methyl orange, Congo red and chromium(VI) by flocculation/adsorption." Carbohydrate Polymers, 2017, Vol. 157, pp. 1568–1576.

10. Du, H., Chen, W., Cai, P., Rong, X., Dai, K., Peacock, C. L., Huang, Q., "Cd(II) Sorption on Montmorillonite-Humic acid-Bacteria Composites." Scientific Reports, 2016, Vol. 6, pp. 1-9.

11. Singh, S., Barick, K. C., Bahadur, D., "Fe_3O_4 embedded ZnO nanocomposites for the removal of toxic metal ions, organic dyes and bacterial pathogens." Journal of Materials Chemistry A, 2013, Vol. 1, pp. 3325–3333.

12. Uzum, C., a, Shahwan, T., Eroglu, A. E., Hallam, K. R., Scott, T. B., Lieberwirth, I. "Synthesis and characterization of kaolinite-supported zero-valent iron nanoparticles and their application for the removal of aqueous Cu^{2+} and Co^{2+} ions." Applied Clay Science, 2009, Vol. 43, pp. 172–181.

13. Karthik, R. and Meenakshi, S., "Removal of Cr(VI) ions by adsorption onto sodiumalginate-polyaniline nanofibers."

International Journal of Biological Macromolecules, 2015, Vol. 72, pp. 711–717.
14. Kumar, S S., Venkateswarlu, P., Rao, V. R., Rao, G. N., "Synthesis, characterization and optical properties of zinc oxide nanoparticles." International Nano Letters, 2013, Vol. 3, pp. 1-6.
15. Langmuir, I., "The adsorption of gases on plane surfaces of glass, mica and platinum." Journal of American Chemical Society, 1918, Vol. 40, pp. 1361-1403.
16. Gueu, S,, Yao, B., Adouby, K., Ado, G., "Kinetics and thermodynamics study of lead adsorption on to activated carbons from coconut and seed hull of the palm tree." International journal of environmental science and technology, 2007, Vol. 4, pp. 11-17.
17. Hall, K. R., Eagleton, L. C., Acrivos, A., Vermeulen, T., "Pore-and solid-diffusion kinetics in fixed-bed adsorption under constant-pattern conditions." Industrial engineering chemistry fundamentals, 1966, Vol. 5, pp. 212-223.
18. Ho Y. S., and McKay, G., "Pseudo-second order model for sorption process." Process biochemistry, 1999, Vol. 34, pp. 451-465.
19. Chehtan, P. D., and Vishalakshi., B., "Synthesis of ethylenediamine modified chitosan microspheres forremoval of divalent and hexavalent ions." International Journal of Biological Macromolecules, 2015, Vol. 75, pp. 179-185.
20. Chethan, P. D., and Vishalakshi, B., "Synthesis of ethylenediamine modified chitosan and evaluation for removal of divalent metal ions." Carbohydrate Polymers, 2013, Vol. 97, pp. 530– 536.
21. Lakshmipathya, R., and Sarada, N. C., "A fixed bed column study for the removal of Pb^{2+} ions by watermelon rind." Environmental Science: Water Research & Technology, 2015, Vol. 1, pp. 244-250.
22. Radi, S., Tighadouini, S., Bacquet, M., Degoutin, S., Janusc, L., Mabkhot, N. Y., "Fabrication and covalent modification of highly chelated hybrid material based on silica-bipyridine framework for efficient adsorption of heavy metals: isotherms, kinetics and thermodynamics studies." RSC Advances, 2016, Vol. 6, pp. 82505-82514.
23. Hmood, A. Y., and Jassim., T. E., "Adsorption of copper(II) and lead ions from aqueous solutions by porcellanite." International Journal of Marine Science, 2015, Vol. 5, pp. 1-7.
24. Kundu, D., Hazra, C., Chatterjee, A., Chaudharia, A., Mishra, S., "Sonochemical synthesis of poly(methyl methacrylate) core–surfactin shell nanoparticles for recyclable removal of heavy metal ions and its cytotoxicity." RSC Advances, 2014, Vol. 4, pp. 24991-25004.
25. Chang, J., Wang, J., Qu, J., Li, Y. V., Ma, L., Wang, L., Wang, X., Pan, K., "Preparation of α-Fe_2O_3/polyacrylonitrile nanofiber mat as an effective lead adsorbent." Environmental Science: Nano, 2016, Vol. 3, pp. 894-901.
26. Onundi, Y. B., Mamun, A. A., Al Khatib, M. F., Ahmed, Y. M., "Adsorption of copper, nickel and lead ions from synthetic semiconductor industrial wastewater by palm shell activated carbon." International Journal of Environmental Science and Technology, 2010, Vol. 7, pp. 751-758.